THE JOURNAL OF PHYSICAL CHEMISTRY B LETTERS

2005, *109,* 19052−19055
Published on Web 09/23/2005

Study of the Morphological and Adhesion Properties of Collagen Fibers in the Bruch's Membrane

Shrestha Basu Mallick[†] and Albena Ivanisevic[*,‡,§]

Department of Physics, Weldon School of Biomedical Engineering, and Department of Chemistry, Purdue University, West Lafayette, Indiana 47907

Received: July 1, 2005; In Final Form: September 8, 2005

The Bruch's membrane is located beneath the retina in vertebrate eyes. We have used atomic force microscopy to examine the morphological and adhesion properties of collagen fibers located in different portions of the membrane. The *D*-periodicity of the fibers was 62.54 ± 4.25 nm and 63.78 ± 4.14 nm for regions away from the optic nerve and close to it, respectively. The adhesion properties of the collagen fibers were evaluated using force volume imaging on a number of different eye samples. The adhesion force we recorded in regions away from the optic nerve was different compared to regions close to the optic nerve. The reported results allow us to understand the nanoscopic properties of connective tissues in the eye and are important for the design of new and improved biomaterials.

Collagen is part of the extracellular matrix and is one of the most abundant structural proteins in different mammalian tissues.[1] A variety of collagen types have been identified. These types vary in the length of their helix and the nature of their nonhelical portions.[2] The various types of collagen are located in different areas and can form large fibrous structures: type I (skin, tendon, bone), type II (cartilage), and type III (skin).[3] The properties of these structures have been studied using a variety of techniques such as immunohistological staining, transmission electron microscopy (TEM), scanning electron microscopy (SEM), and X-ray diffraction. The emergence of the atomic force microscope (AFM) as a useful tool for biologists has provided insight into the periodic structure and characteristics of collagen in bone, tendon, skin, and cartilage.[3−8] In addition to in vitro AFM morphological studies, this technique has been used to determine the mechanical properties of isolated collagen,[9,10] to detect the binding and cleavage sites of collagenases,[11] to quantify antibody−antigen interactions on collagen,[4] to nanodissect such fibers,[12] and to manipulate the assembly of collagen matrixes.[13]

Collagen is also found in eye tissues. AFM has been used to image isolated fibers from cornea and sclera.[14−16] In addition, modifications resulting from laser ablation in corneal stroma were investigated by AFM.[17] Miyagama et al. have also reported the surface ultrastructure of collagen fibrils and their association with proteoglycans in the cornea and the sclera using AFM.[18,19] Such studies have shown the usefulness of AFM in terms of understanding the distribution of collagen in mammalian ocular tissues. In this study, we report the morphological and adhesion properties of collagen fibers in the Bruch's membrane. The Bruch's membrane is a thin, compact layer of fibers located just beneath the retina.

To the best of our knowledge, no comprehensive studies in the literature have investigated the topography and adhesion properties of the Bruch's membrane using AFM. Understanding the properties of collagen fibers in this membrane is essential in trying to design better biomaterials to help patients who suffer from eye disorders such as age-related macular degeneration.[20] With this disease, considerable morphological and hence mechanical changes are expected in the Bruch's membrane.[21] These changes have been hypothesized to be related to alterations in the collagen fibers within the membrane. Therefore, designing strategies to map and rationalize the collagenous material's properties at the nanometer scale is important to advancing our understanding of how to help patients with eye problems. In this work, we use AFM to compare and contrast the morphology and the adhesion characteristics of collagen fibers extracted from different parts of the Bruch's membrane.

Eyes were obtained from euthanized pigs. The diameters of the eyeballs used were not always identical because of differences in the sizes and ages of the animals. The eyes were carefully enucleated and stored in phosphate-buffered saline at 4 °C. The dissection of the eyes was performed on the basis of established methods.[22] The membrane samples were sliced into smaller pieces, attached to the AFM holder, and air-dried. All other parts of the eyes were not used for this study. All AFM measurements were performed using a Multi-Mode Nanoscope IIIa (Veeco Instruments) equipped with a Nanoscope Software System. For all experiments, the AFM was in an environmental chamber where the temperature was 20−22 °C and the humidity was 21−33%. The force constants for the cantilevers used (model #OTESPA7, Veeco Instruments) were around 37 N/m and were determined using a literature procedure.[23] All adhesion studies were done in force volume (FV) mode. FV images were generally collected at a *Z* travel distance of 150 nm with a

* To whom correspondence should be addressed. albena@purdue.edu.
[†] Department of Physics.
[‡] Weldon School of Biomedical Engineering.
[§] Department of Chemistry.

10.1021/jp053605w CCC: $30.25

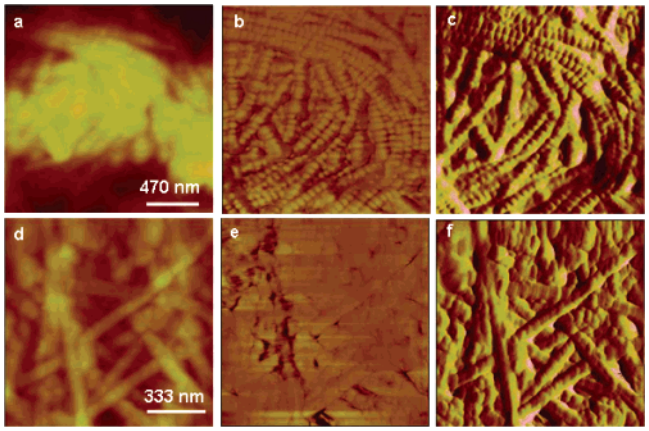

Figure 1. Tapping-mode AFM images in air. Height (a), phase (b), and amplitude (c) images for a region away from the optic nerve. Height (d), phase (e), and amplitude (f) images for a region close to the optic nerve.

sample number of 16 points per force curve. For every FV image, 128 sample points per line were obtained. We used the trigger mode to eliminate the system's drift. In addition to FV images, topography images were collected simultaneously at 256 sample points per line. All experiments reported in this study were done in two steps: Initially, a regular tapping-mode image was collected in a selected area. Subsequently, the FV imaging, which collects a FV map and an independent height image, was performed. If there is no drift in the system and the resolution in the FV mode is sufficiently high, at the end of the two steps experiment one obtains two height images that look almost identical.

We systematically examined samples extracted from regions away from the optic nerve and close to it. We recorded the morphology of the samples using both contact-mode and tapping-mode imaging. We verified that we are not damaging the dried tissue in contact mode. The data collected in both imaging modes was similar. Typical images recorded for the two regions are shown in Figure 1. The data indicates that the collagen fibers were interwoven in collagenous layers. We prepared the samples in our studies with care to preserve as much as possible the original architecture of the membrane. A number of researchers have looked at the properties of isolated collagen fibers from eye tissues.[15] Such samples are prepared by making collagen suspensions from the appropriate tissue and subsequently spreading the fibers on solid supports. In contrast, during our experiments, steps were taken not to disturb the original arrangement of the collagen fibers. This preparation method led to samples with uneven surface features. Such uneven surface features can increase convolution effects as the tip scans across the surface and examines areas with variable sizes. We took a quantitative approach in trying to assess possible variation in the morphology of the fibers from the two types of samples rather than looking at contrast differences or assessing visual appearances. The Supporting Information includes all the images we collected. All the images were analyzed and represent a statistically significant number of eye samples. We acquired high-resolution images where individual fibers were clearly visible in regions away from and close to the optic nerve. We measured the longitudinal profiles of individual fibers on our images and compared the results we obtained with previous data. We assessed the *D*-periodicity that is associated with the periodic grooves and ridges as well as the groove depth. The groove depth is defined as the difference in height between the grooves and the ridges. The average *D*-periodicity was 62.54 ± 4.25 nm and 63.78 ± 4.14 nm for samples away from the optic nerve and close to the optic nerve, respectively. These ranges of *D*-periodicities are in agreement with values reported for collagen extracted from cornea and sclera samples.[14,15] The groove depth was calculated to be 3.88 ± 1.32 nm and 2.73 ± 1.07 nm for regions away from the optic nerve and close to it, respectively. Literature reports indicate different values for the groove depth.[15,16] Researchers have pointed out that differences may be due to age variations of experimental animals and preparation artifacts such as deformation during the air-drying process. High-resolution morphological studies are not sufficient to record possible differences among collagen types located in different regions of the Bruch's membrane.

Histology studies have reported that the distribution of collagen types in the Bruch's membrane varies in its different regions. On the basis of these studies, we hypothesize that the fibers observed in Figure 1a,d can be of different collagen types. One cannot distinguish among the different types of collagen just from the *D*-periodicity obtained from the high-resolution images, because a number of the expected collagen types have similar repeating units. Experiments have shown the presence of collagen types I−VI in the Bruch's membrane.[20] In particular, detailed investigation regarding the presence of isoforms of collagen IV and VI in the Bruch's membrane have been shown to contribute to the age-related thickening of this membrane.[24−26] However, none of these studies have been able to correlate the identity of the collagen with its adhesion characteristics. As shown above, high-resolution morphological studies alone are not enough to distinguish among different types of collagen. However, correlating the adhesion properties with morphological and histological studies is important when assessing changes that can lead to eye diseases associated with age-related degeneration in the tissues.

One needs to preserve the original arrangement of the membrane components as much as possible in order to gain an understanding of how adhesion properties correlate with previously reported histological studies and morphological characteristics. We have attempted to image the membranes in solution using AFM. In solution, the sheets formed by the collagenous fibers are fluid. Therefore, getting a stable image of them was not possible because of the constant movement of the fibers. Other researchers have shown that isolated collagen fibers can be firmly anchored on solid supports in order to obtain stable AFM images in fluid.[5] AFM adhesion studies in fluid will provide more physiologically relevant information but will require some sort of a fixing protocol[4] that will result in the alteration of the original arrangement of the different types of collagen. Therefore, we chose to perform the adhesion studies in air in order to assess changes in adhesion characteristics between the two different regions extracted from the Bruch's membrane. Our protocol does not allow us to extract physiologically relevant quantitative information. The FV measurements in air can allow one to look at gradients with different hydrophobicities. Other researchers have used this method to extract variations across Langmuir−Blodgett films and have validated the origin of the adhesion forces.[27] Our studies are important in terms of mapping relative differences and making qualitative comparisons. The adhesion mapping described below can be applied to clinically relevant samples and help in the identification of changes in the properties and the composition of the membrane in patients with age-related diseases.

The adhesion properties of the two different regions were investigated using FV imaging. We looked at a number of samples from each region. We looked at areas where only

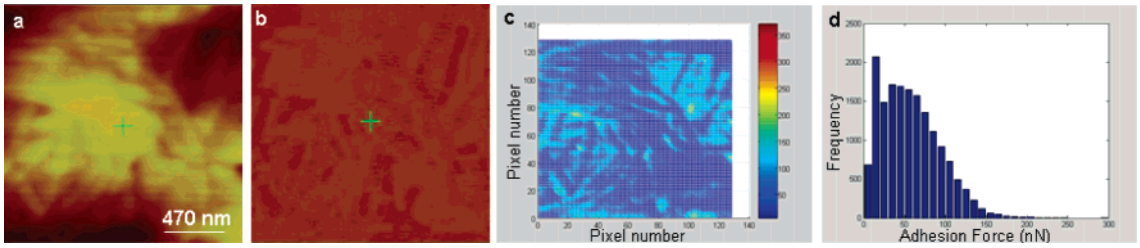

Figure 2. Topography (a) and an FV image (b) of an area away from the optic nerve. Part c is the adhesion map for the data from part b. The color *z* scale is in nanonewtons. Part d is a histogram showing the distribution of forces extracted from the FV image in part b.

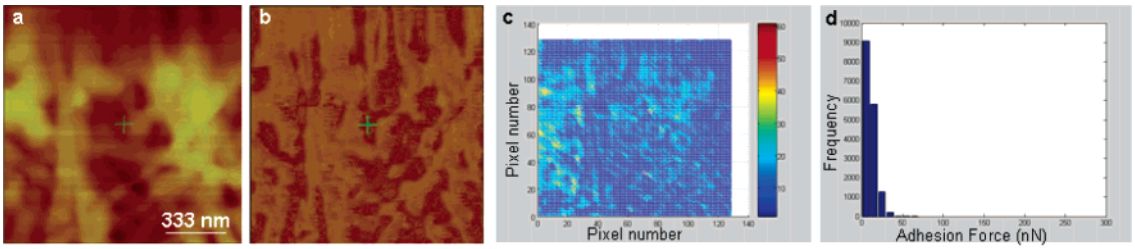

Figure 3. Topography (a) and an FV image (b) of an area close to the optic nerve. Part c is the adhesion map for the data from part b. The color *z* scale is in nanonewtons. Part d is a histogram showing the distribution of forces extracted from the FV image in part b.

TABLE 1: Average Adhesion Forces for Each Sample Type

sample type	average adhesion force (nN)	number of FV images	total number of force curves
away from the optic nerve	42.52 ± 24.83	12	196 608
close to the optic nerve	14.47 ± 6.22	9	147 456

collagen fibers were present. The data acquired for representative regions away from the optic nerve and close to it are shown in Figures 2 and 3, respectively. Parts A of these figures show topography images acquired in the FV mode with a resolution of 256 × 256 pixels. Parts B of the two figures show the FV images collected simultaneously with the height images. The individual pixels in the FV image correspond to an individual force curve. Each FV image we collected was composed of 16 384 force curves. The adhesion maps displayed in parts C of Figures 2 and 3 were calculated using the data of the FV images and analyzed using custom-written MatLab code. The code was designed to extract the data utilizing approaches reported in the literature.[28,29] Parts D of Figures 2 and 3 show histograms that correspond to the distribution of adhesion forces necessary to detach the clean AFM tip from the sample extracted away from the optic nerve and that close to it, respectively. The histograms display a range of adhesion forces. The range can be influenced by the contact area, the topography of the sample, and the nature of chemical species present on the surface.

Our results indicate that there is a difference in adhesion force between the clean tip and the two areas of the membrane. Additional data is presented in the Supporting Information. Table 1 summarizes the average values for each region. Previous work has shown that the arithmetic mean is not an appropriate measure to utilize for the understanding of differences in the interaction of a tip with a given surface.[28] The various data sets displayed in the paper and the Supporting Information were collected with different tips, and therefore, the contact area between the tip and the sample was varied. A way to account for differences is to divide the mean adhesion force by the radius of the tip. This method has been used to correct the forces with respect to contact area between the tip and the sample.[28] After acquiring FE-SEM images and comparing the various areas of tip contacts, we still observe the above trends. In all of our FV studies, we looked only for samples with densely packed collagen. This allowed us to compare the various histograms we generated, since they represent adhesion only to the collagen fibers, regardless of the size of the imaging area (see Supporting Information for additional data). The measurements done in air can account for differences in adhesion forces due to the variability in hydrophobicities of the sample features. One expects the largest force from the interaction of two hydrophilic surfaces of the same kind (e.g., −OH group on the surface of the tip interacting with an −OH group on the surface of the tissue).[30] It is important to note that the observed differences in adhesion can result from the variable distribution of collagen fibers in the selected area. In our experiments, these differences in adhesion, despite similar topography, can also be explained by what is known about the chemical structure of the two regions. The macula surrounds the area adjacent to the optic nerve. The area around the optic nerve is thicker. Histological studies have shown that the distribution of collagen types in the Bruch's membrane of the macula is different from other regions.[22] Researchers have observed a preponderance of type III collagen in the macular region of the Bruch's membrane and type VI collagen in the elastic layer of the extramacular region.[20] In terms of characteristics that might influence adhesion properties, the individual types of collagen differ in the number and the nature of carbohydrate attachments to their triple helical structure.[2] Type VI collagen is a heterotrimer that consists of three different α chains.[31] Type III collagen is a homotrimer that can form mixed fibrils with type I collagen.[32] Type I collagen is known to provide tensile stiffness and can influence a number of biomechanical properties such as adhesion.[33] In principle, the differences we observed can also be due to the areas selected for imaging. However, data extracted from different donor eyes and randomly selected areas close to and away from the optic nerve always showed the same trend in adhesion properties. Our results so far show qualitative differences between the two regions that can be explained on the basis of what is known about variations in collagen types in eye tissues. However, AFM imaging coupled with FV mapping can allow one to extract a quantitative distribution of the various types of collagen with a resolution better than that of optical microscopy. To accomplish this, we plan to modify AFM tips with different functional groups and look for specific vs

nonspecific interactions on the basis of the known chemical structure of each collagen type. These experiments are underway in our laboratory.

In summary, we report the morphological characteristics of collagen fibers extracted from two different regions of the Bruch's membrane. The height AFM images and analysis showed no appreciable differences in the appearance of the two regions. FV imaging allowed us to map the adhesion differences between areas away from the optic nerve and close to it. The adhesion was higher in areas away from the optic nerve. The differences can be attributed to the variable distribution of several collagen types in the Bruch's membrane. The methodology we report allows one to map properties of eye tissues at the nanometer scale. These properties are important when trying to understand how age-related changes in the eye tissues contribute to the development of diseases that can lead to blindness.

Acknowledgment. This work was supported by the Bindley Biosciences Center at Purdue. We thank the veterinary staff of the Weldon School of Biomedical Engineering for extracting the eyes after pig surgeries.

Supporting Information Available: Supporting figures provide more details regarding the analysis of all samples. This material is available free of charge via the Internet at http://pubs.acs.org.

References and Notes

(1) Lin, A. C.; Goh, M. C. *Proteins: Struct., Funct., Genet.* **2002**, *49*, 378−384.

(2) Ogawa, M.; Moody, M. W.; Portier, R. J.; Bell, J.; Schexnayder, M. A.; Losso, J. N. *J. Agric. Food Chem.* **2003**, *51*, 8088−8092.

(3) Gutsmann, T.; Fantner, G. E.; Venturoni, M.; Nkodo, A. E.; Thompson, J. B.; Kindt, J. H.; Morse, D. E.; Fygenson, D. K.; Hansma, P. K. *Biophys. J* **2003**, *84*, 2593−2598.

(4) Avci, R.; Schweitzer, M.; Boyd, R. D.; Wittmeyer, J.; Steele, A.; Toporski, J.; Beech, I.; Arce, F. T.; Spangler, B.; Cole, K. M.; McKay, D. S. *Langmuir* **2004**, *20*, 11053−11063.

(5) Graham, J. S.; Vomund, A. N.; Phillips, C. L.; Grandbois, M. *Exp. Cell Res.* **2004**, *299*, 335−342.

(6) Chernoff, E. A. G.; Chernoff, D. A. *J. Vac. Sci. Technol., A* **1992**, *10*, 596−599.

(7) Paige, M. F.; Rainey, J. K.; Goh, M. C. *Micron* **2001**, *32*, 341−353.

(8) Avci, R.; Schweitzer, M. H.; Boyd, R. D.; Wittmeyer, J. L.; Arce, F. T.; Calvo, J. O. *Langmuir* **2005**, *21*, 3584−3590.

(9) Dufrene, Y. F.; Thibault, G. M.; Rouxhet, P. G. *Langmuir* **1999**, *15*, 2871−2878.

(10) Dupont-Gillain, C. C.; Jacquemart, I. *Surf. Sci.* **2003**, *539*, 145−154.

(11) Sun, H. B.; Smith, G. N., Jr.; Hasty, K. A.; Yokota, H. *Anal. Biochem.* **2000**, *283*, 153−158.

(12) Wen, C. K.; Goh, M. C. *Nano Lett.* **2003**, *4*, 129−132.

(13) Kim, H.; Arakawa, H.; Osada, T.; Ikai, A. *Appl. Surf. Sci.* **2002**, *188*, 493−498.

(14) Yamamoto, S.; Hitomi, J.; Sawaguchi, S.; Abe, H.; Shigeno, M.; Ushiki, T. *Jpn. J. Ophthalmol.* **2002**, *46*, 496−501.

(15) Yamamoto, S.; Hitomi, J.; Shigeno, M.; Sawaguchi, S.; Abe, H.; Ushiki, T. *Arch. Histol. Cytol.* **1997**, *60*, 371−378.

(16) Meller, D.; Peters, K.; Meller, K. *Cell Tissue Res.* **1997**, *288*, 111−118.

(17) Lydataki, S.; Lesniewska, E.; Tsilimbaris, M. K.; Panagopoulou, S.; Le Grimellec, C.; Pallikaris, I. G. *Single Mol.* **2002**, *3*, 141−147.

(18) Miyagawa, A.; Kobayashi, M.; Fujita, Y.; Nakamura, M.; Hirano, K.; Kobayashi, K.; Miyake, Y. *Jpn. J. Ophthalmol.* **2000**, *44*, 591−595.

(19) Miyagawa, A.; Kobayashi, M.; Fujita, Y.; Hamdy, O.; Hirano, K.; Nakamura, M.; Miyake, Y. *Cornea* **2001**, *20*, 651−656.

(20) Marshall, G. E.; Konstas, A. G. P.; Reid, G. G.; Edwards, J. G.; Lee, W. R. *Graefes Arch. Clin. Exp. Ophthalmol.* **1994**, *232*, 133−140.

(21) Guymer, R.; Luthert, P.; Bird, A. *Prog. Retinal Eye Res.* **1998**, *18*, 59−90.

(22) Karwatowski, W. S. S.; Jeffries, T. E.; Duance, V. C.; Albon, J.; Bailey, A. J.; Easty, D. L. *Br. J. Ophthalmol.* **1995**, *79*, 944−952.

(23) Poggi, M. A.; McFarland, A. W.; Colton, J. S.; Bottomley, L. A. *Anal. Chem.* **2004**.

(24) Chen, L.; Miyamura, N.; Ninomiya, Y.; Handa, J. T. *Br. J. Ophthalmol.* **2003**, *87*, 212−215.

(25) Marshall, G. E.; Konstas, A. G. P.; Reid, G. G.; Edwards, J. G.; Lee, W. R. *Br. J. Ophthalmol.* **1992**, *76*, 607−614.

(26) Knupp, C.; Amin, S. Z.; Munro, P. M. G.; Luthert, P. J.; Squire, J. M. *J. Struct. Biol.* **2002**, *139*, 181−189.

(27) van der Warf, K. O.; Putman, C. A. J.; de Grooth, B. G.; Greve, J. *Appl. Phys. Lett.* **1994**, *65*, 1195−1197.

(28) Poggi, M. A.; Bottomley, L. A.; Lillehei, P. T. *Nano Lett.* **2004**, *4*, 61−64.

(29) Eaton, P.; Smith, J. R.; Graham, P.; Smart, J. D.; Nevell, T. G.; Tsibouklis, J. *Langmuir* **2002**, *18*, 3387−3389.

(30) Grinevich, O.; Mejiritski, A.; Neckers, D. C. *Langmuir* **1999**, *15*, 5, 2077−2079.

(31) Chu, M. L.; Mann, K. H.; Deutzmann, R.; Pribula-Conway, D.; Hsu-Chen, C. C.; Bernard, M. P.; Timpl, R. *Eur. J. Biochem.* **1987**, *168*, 309−317.

(32) Gelse, K.; Poschl, E.; Aigner, T. *Adv. Drug Delivery Rev.* **2003**, *55*, 1531−1546.

(33) Hulmes, D. J.; Miller, A. *Nature (London)* **1981**, *293*, 234−239.